

# A Theoretically Grounded Application of Dropout in Recurrent Neural Networks

Yarin Gal

University of Cambridge

YG279@CAM.AC.UK

## Abstract

Recurrent neural networks (RNNs) stand at the forefront of many recent developments in deep learning. Yet a major difficulty with these models is their tendency to overfit. Dropout is a widely used tool for regularisation in deep models, but a long strand of *empirical* research has claimed that it cannot be applied between the recurrent connections of an RNN. The argument is that noise hinders the network’s ability to model sequences and therefore dropout should be applied to the RNN’s inputs and outputs alone. But without regularisation in recurrent layers, existing techniques overfit quickly. In this paper we make use of a recently developed theoretical framework casting dropout as approximate variational inference. Based on the framework we derive *mathematically grounded* tools to apply dropout within the recurrent layers of RNNs, eliminating model overfitting. We apply our new variational inference based dropout technique in LSTM and GRU networks, evaluating the technique empirically. We show that the new approach outperforms existing techniques on sentiment analysis and language modelling tasks, extending our arsenal of variational tools in deep learning.

## 1. Introduction

Recurrent neural networks (RNNs) are sequence-based models of key importance in natural language understanding, language generation, video processing, and many other tasks (Sundermeyer et al., 2012; Kalchbrenner & Blunsom, 2013; Sutskever et al., 2014). The model’s input is a sequence of symbols, where at each time step a simple network (*RNN unit*) is applied to a single symbol together with the network’s output from the previous time step. RNNs are powerful models, but can overfit and pose special difficulties when faced with small data. Dropout is a popular regularisation technique with deep networks (Hinton et al., 2012; Srivastava et al., 2014), but the technique has never been applied successfully to RNNs’ recurrent layers (connections between time steps). Empirical results led many to believe that noise added to recurrent layers will be amplified for long sequences, and drown the signal (Zaremba,

Sutskever, and Vinyals, 2014). Through a process of empirical experimentation, it was thus suggested to use the technique with the inputs and outputs of the RNN alone (Pachitariu & Sahani, 2013; Bayer et al., 2013; Pham et al., 2014; Zaremba et al., 2014; Bluche et al., 2015). But the lack of regularisation in recurrent layers leaves the model susceptible to overfitting, only deferring the problem.

Contrary to existing *experimental* results, we propose a new approach that can be applied to the recurrent connections successfully, built on solid *theoretical* developments. This allows us to train RNNs on small data, and improve model performance with large data. We rely on recent theoretical results which showed that many stochastic training techniques in deep learning follow the same mathematical foundations as approximate inference in Bayesian neural networks (NNs). Dropout, for example, is equivalent to approximate variational inference with Bernoulli variational distributions (Gal & Ghahramani, 2015a). Models such as convolutional neural networks have gained a considerable boost in performance following this Bayesian interpretation. Further, this view offers uncertainty estimates reflecting the models’ confidence in their outputs (Gal & Ghahramani, 2015b).

Building on these theoretical developments we introduce new *approximate inference techniques* in Bayesian RNNs – RNNs with network weights treated as random variables. Approximating the posterior distribution over the weights with a Bernoulli approximating variational distribution reveals how dropout should be applied in RNNs. More specifically, the random weights when conditioned on observations have a posterior. This posterior is approximated with a Bernoulli approximating distribution. Implementing this approximate inference procedure is identical to performing dropout in the RNN. Following this approach, one would repeat the same dropout mask at each time step for both inputs, outputs, and recurrent connections – in contrast to existing techniques where different dropout masks would be sampled at each time step for the inputs and outputs alone. When used with discrete inputs (i.e. words) we place a distribution over the word embeddings as well – resulting in a fully Bayesian model. Approximate inference in the word-based model corresponds to randomly dropping words in the sentence, and might be interpreted as forcing the model not to rely on single words for its task.

The new approach manages to avoid overfitting while improving model accuracy. We demonstrate the technique with a sentiment analysis task, where labelled data is scarce and has to be hand-annotated (Pang & Lee, 2005). We study the proposed approach through an extensive array of experiments under different conditions and for different RNN structures (both LSTM and GRU networks), and show significant improvement in perplexity on a language modelling benchmark compared to existing approaches. Full code and experiment setups (for reproducibility) is available online at <http://yarin.co/BRNN>.

## 2. Background

We review necessary background in recurrent neural networks, Bayesian neural networks, and their relation to dropout. We will build on these ideas in the next section, proposing approximate inference in the Bayesian RNN.

### 2.1. Dropout

Let  $\hat{\mathbf{y}}$  be the output of a NN with  $L$  layers and a loss function  $E(\cdot, \cdot)$  (such as the softmax loss or the Euclidean loss). We denote by  $\mathbf{W}_i$  the NN's weight matrices of dimensions  $K_i \times K_{i-1}$ , and by  $\mathbf{b}_i$  the bias vectors of dimensions  $K_i$  for each layer  $i = 1, \dots, L$ . The NN defines a function

$$\hat{\mathbf{y}} = \mathbf{f}^\omega(\mathbf{x}) := \mathbf{h}^{\mathbf{W}_L, \mathbf{b}_L}(\dots \mathbf{h}^{\mathbf{W}_1, \mathbf{b}_1}(\mathbf{x}) \dots)$$

for  $\mathbf{h}^{\mathbf{W}, \mathbf{b}}(\mathbf{x}) = \sigma(\mathbf{x}\mathbf{W} + \mathbf{b})$ , parametrised by  $\omega = \{\mathbf{W}_i, \mathbf{b}_i\}_{i=1}^L$ . The elements of the vector  $\mathbf{h}^{\mathbf{W}, \mathbf{b}}(\mathbf{x})$  are the *network units*. During NN optimisation a regularisation term is often used. We often use  $L_2$  regularisation weighted by some weight decay  $\lambda$ , resulting in a minimisation objective (often referred to as cost),

$$\mathcal{L} := \frac{1}{N} \sum_{i=1}^N E(\mathbf{y}_i, \hat{\mathbf{y}}_i) + \lambda \sum_{i=1}^L (\|\mathbf{W}_i\|_2^2 + \|\mathbf{b}_i\|_2^2). \quad (1)$$

With dropout, we sample binary variables for every input point and for every network unit in each layer. Each binary variable takes value 1 with probability  $p_i$  for layer  $i$ . A unit is dropped (i.e. its value is set to zero) for a given input if its corresponding binary variable takes value 0. We use the same binary variable values in the backward pass propagating the derivatives to the parameters. At test time we might use MC dropout (Srivastava et al., 2014; Gal & Ghahramani, 2015b) by averaging stochastic forward passes through the network. An approximation to this could be obtained by replacing the weights  $\mathbf{W}_i$  by  $p_i \mathbf{W}_i$ , and performing a normal deterministic pass through the network (Srivastava et al., 2014). This approximation is often used in the literature with deep models.

### 2.2. Recurrent Neural Networks

A recurrent NN is a specialised network for sequence data. Given an input sequence  $\mathbf{x} = [\mathbf{x}_1, \dots, \mathbf{x}_T]$  of length  $T$ , an

RNN can be written as a repeated application of two functions  $\mathbf{f}_c^\omega, \mathbf{f}_y^\omega$  multiple times. These generate the internal state  $\mathbf{c}_t$  and the output  $\mathbf{y}_t$  at each time step  $t$ :

$$\begin{aligned} \mathbf{c}_t &= \mathbf{f}_c^\omega(\mathbf{x}_t, \mathbf{y}_{t-1}, \mathbf{c}_{t-1}) \\ \mathbf{y}_t &= \mathbf{f}_y^\omega(\mathbf{x}_t, \mathbf{y}_{t-1}, \mathbf{c}_t). \end{aligned}$$

These can be composed in hierarchies to create deep RNNs. For example, a long short-term memory RNN (LSTM, Hochreiter & Schmidhuber, 1997) is defined by setting

$$\begin{aligned} \mathbf{i} &= \sigma(\mathbf{y}_{t-1}\mathbf{U}_i + \sigma(\mathbf{x}_t\mathbf{W}_i)) \\ \mathbf{f} &= \sigma(\mathbf{c}_{t-1}\mathbf{U}_f + \sigma(\mathbf{x}_t\mathbf{W}_f)) \\ \mathbf{f}_c^\omega(\mathbf{x}_t, \mathbf{y}_{t-1}, \mathbf{c}_{t-1}) &= \mathbf{f} \circ \mathbf{c}_{t-1} + \mathbf{i} \circ \sigma(\mathbf{y}_{t-1}\mathbf{U}_c + \sigma(\mathbf{x}_t\mathbf{W}_c)) \\ \mathbf{f}_y^\omega(\mathbf{x}_t, \mathbf{y}_{t-1}, \mathbf{c}_t) &= \sigma(\mathbf{y}_{t-1}\mathbf{U}_y + \sigma(\mathbf{x}_t\mathbf{W}_y)) \circ \sigma(\mathbf{c}_t) \end{aligned}$$

with  $\omega = \{\mathbf{W}_f, \mathbf{U}_f, \mathbf{W}_i, \mathbf{U}_i, \mathbf{W}_c, \mathbf{U}_c, \mathbf{W}_y, \mathbf{U}_y\}$  weight matrices,  $\sigma$  element-wise non-linearity, and  $\circ$  the element-wise product. Here the internal state  $\mathbf{c}_t$  (also referred to as *cell*) is updated additively. The weight matrices  $\mathbf{W}_f, \mathbf{U}_f$  are often interpreted as “forget” gates, with  $\mathbf{W}_i, \mathbf{U}_i, \mathbf{W}_y, \mathbf{U}_y$  interpreted as input and output gates correspondingly. An alternative popular RNN structure, known as a gated recurrent unit network (GRU, Cho et al., 2014), offers a simpler formulation:

$$\begin{aligned} \mathbf{z} &= \sigma(\mathbf{y}_{t-1}\mathbf{U}_z + \mathbf{x}_t\mathbf{W}_z) \\ \mathbf{r} &= \sigma(\mathbf{y}_{t-1}\mathbf{U}_r + \mathbf{x}_t\mathbf{W}_r) \\ \mathbf{f}_y^\omega(\mathbf{x}_t, \mathbf{y}_{t-1}) &= \mathbf{z} \circ \mathbf{y}_{t-1} + (\mathbf{1} - \mathbf{z}) \circ \sigma(\mathbf{x}_t\mathbf{W}_h + \mathbf{r} \circ \mathbf{y}_{t-1}\mathbf{U}_h) \end{aligned}$$

with weight matrices  $\omega = \{\mathbf{W}_z, \mathbf{U}_z, \mathbf{W}_r, \mathbf{U}_r, \mathbf{W}_h, \mathbf{U}_h\}$  and  $\mathbf{1}$  being a vector of 1's. When applying dropout to either model, existing techniques will randomly set to zero elements of the vector  $\mathbf{x}_t$  only. For hierarchical models (where  $\mathbf{y}_t$  is used as the input to another RNN), random elements of  $\mathbf{y}_t$  will be set to zero only when  $\mathbf{y}_t$  is used as input to the next RNN.

### 2.3. Bayesian Neural Networks

Given training inputs  $\mathbf{X} = \{\mathbf{x}_1, \dots, \mathbf{x}_N\}$  and their corresponding outputs  $\mathbf{Y} = \{\mathbf{y}_1, \dots, \mathbf{y}_N\}$ , in Bayesian regression we would like to estimate a function  $\mathbf{y} = \mathbf{f}(\mathbf{x})$  that is *likely to have generated* our outputs. What is a function that is likely to have generated our data? Following the Bayesian approach we would put some *prior* distribution over the space of functions,  $p(\mathbf{f})$ . This distribution represents our prior belief as to which functions are likely to have generated our data. We then look for the *posterior* distribution over the space of functions given our dataset:  $p(\mathbf{f}|\mathbf{X}, \mathbf{Y})$ . This distribution captures the most likely functions given our observed data. With it we can predict an output for a new input point  $\mathbf{x}^*$  by integrating

$$p(\mathbf{y}^*|\mathbf{x}^*, \mathbf{X}, \mathbf{Y}) = \int p(\mathbf{y}^*|\mathbf{f}^*)p(\mathbf{f}^*|\mathbf{x}^*, \mathbf{X}, \mathbf{Y})d\mathbf{f}^*. \quad (2)$$

One way to define a distribution over functions is to place a prior distribution over a NN's weights, resulting in a *Bayesian NN*. Given weight matrices  $\mathbf{W}_i$  and bias vectors  $\mathbf{b}_i$  for layer  $i$ , we often place standard matrix Gaussian prior distributions over the weight matrices,  $p(\mathbf{W}_i)$ :

$$\mathbf{W}_i \sim \mathcal{N}(\mathbf{0}, \mathbf{I})$$

and often assume a point estimate for the bias vectors for simplicity. Denote the random output of a NN with (now random) weight matrices  $\omega$  on input  $\mathbf{x}$  by  $\mathbf{f}^\omega(\mathbf{x})$ , and the output over dataset  $\mathbf{X}$  by  $\mathbf{F} = [\mathbf{f}^\omega(\mathbf{x}_1), \dots, \mathbf{f}^\omega(\mathbf{x}_N)]$ . We assume a likelihood<sup>1</sup>  $p(\mathbf{y}|\mathbf{x}, \omega) = \int p(\mathbf{y}|\mathbf{f})p(\mathbf{f}|\mathbf{x}, \omega)d\mathbf{f}$ . For classification tasks we may assume a softmax likelihood given the NN's random output  $\mathbf{f}^\omega = \mathbf{f}^\omega(\mathbf{x})$ :

$$p(\mathbf{y}|\mathbf{f}^\omega) = \text{Categorical} \left( \exp(\mathbf{f}^\omega) / \sum_{d'} \exp(f_{d'}^\omega) \right)$$

or a Gaussian likelihood for regression:

$$p(\mathbf{y}|\mathbf{f}^\omega) = \mathcal{N}(\mathbf{y}; \mathbf{f}^\omega, \tau^{-1} \mathbf{I})$$

with model precision  $\tau$  (see Gal & Ghahramani (2015b) for more details).

#### 2.4. Approximate Inference in Bayesian Neural Networks and Dropout

We are interested in finding the function distribution (or, when dealing with Bayesian NNs, the weight matrices parametrising the functions) that has generated our data. This is the posterior over the weights given our observables  $\mathbf{X}, \mathbf{Y}$ :  $p(\omega|\mathbf{X}, \mathbf{Y})$ . This posterior is not tractable in general, and we use variational inference to approximate it as was done in (Hinton & Van Camp, 1993; Barber & Bishop, 1998; Graves, 2011; Blundell et al., 2015). We need to define an approximating variational distribution  $q(\omega)$ , and then minimise the KL divergence between the approximating distribution and the full posterior:

$$\begin{aligned} \text{KL}(q(\omega)||p(\omega|\mathbf{X}, \mathbf{Y})) &\propto \\ &- \int q(\omega) p(\mathbf{F}|\mathbf{X}, \omega) \log p(\mathbf{Y}|\mathbf{F}) d\mathbf{F} d\omega + \text{KL}(q(\omega)||p(\omega)) \\ &= - \sum_{i=1}^N \int q(\omega) \log p(\mathbf{y}_i|\mathbf{f}^\omega(\mathbf{x}_i)) d\omega + \text{KL}(q(\omega)||p(\omega)). \end{aligned} \quad (3)$$

See (Gal & Ghahramani, 2015b) for a full derivation. We define our approximating variational distribution  $q(\omega) = \prod q(\mathbf{W}_i)$  and for every layer  $i$ ,

$$\begin{aligned} \mathbf{W}_i &= \text{diag}([z_{i,j}]_{j=1}^{K_i}) \cdot \mathbf{M}_i \\ z_{i,j} &\sim \text{Bernoulli}(p_i) \text{ for } i = 1, \dots, L, j = 1, \dots, K_{i-1} \end{aligned} \quad (4)$$

<sup>1</sup>A usual assumption is for  $p(\mathbf{f}|\mathbf{x}, \omega)$  to be a delta function at the network output on  $\mathbf{x}$  given random weights  $\omega$ .

with  $z_{i,j}$  Bernoulli distributed random variables. We optimise over the variational parameters  $\theta = \{\mathbf{M}_i\}_{i=1}^L$  (which will correspond to the NN's weight matrices). Approximating eq. (3) with Monte Carlo integration over  $\omega$  we obtain a noisy objective. This is the same objective as the one used during dropout training: sampling  $\omega$  is identical to sampling Bernoulli random variables  $z_{i,j}$  with probability  $p_i$  – which is identical to randomly setting row  $j$  of  $\mathbf{M}_i$  to zero. Implementing this approximate Bayesian NN inference as a computer program, and implementing dropout in deep networks, would result in identical code for network training (Gal & Ghahramani, 2015a).

Predictions in this model can be approximated with

$$\begin{aligned} p(\mathbf{y}^*|\mathbf{x}^*, \mathbf{X}, \mathbf{Y}) &\approx \int p(\mathbf{y}^*|\mathbf{x}^*, \omega) q(\omega) d\omega \\ &\approx \frac{1}{T} \sum_{t=1}^T p(\mathbf{y}^*|\mathbf{x}^*, \hat{\omega}_t) \end{aligned} \quad (5)$$

with  $\hat{\omega}_t \sim q(\omega)$ , i.e. by performing dropout at test time and averaging the results, referred to as MC dropout.

### 3. Bayesian Recurrent Neural Networks

We now develop approximate inference for Bayesian RNNs, extending the result from the previous section to recurrent networks. A Bayesian RNN is built by placing a prior distribution over the weight matrices  $\omega$  of an RNN (for example  $\omega = \{\mathbf{W}_f, \mathbf{U}_f, \mathbf{W}_i, \mathbf{U}_i, \mathbf{W}_c, \mathbf{U}_c, \mathbf{W}_y, \mathbf{U}_y\}$  for an LSTM or  $\omega = \{\mathbf{W}_z, \mathbf{U}_z, \mathbf{W}_r, \mathbf{U}_r, \mathbf{W}_h, \mathbf{U}_h\}$  for GRU), making these into random variables<sup>2</sup>. To perform approximate inference in the model we need to minimise  $\text{KL}(q(\omega)||p(\omega|\mathbf{X}, \mathbf{Y}))$  given  $q(\omega)$ . Following the derivations in the previous section, we obtain an optimisation objective as in eq. (3). Evaluating each sum term in the equation with our special  $\mathbf{f}$  structure on  $\mathbf{x} = [\mathbf{x}_1, \dots, \mathbf{x}_T]$  and corresponding outputs<sup>3</sup>  $\mathbf{y} = [\mathbf{y}_0, \mathbf{y}_1, \dots, \mathbf{y}_T]$  we obtain

$$\begin{aligned} &\int q(\omega) \log p(\mathbf{y}_T|\mathbf{f}_y^\omega(\mathbf{x}_T, \mathbf{y}_{T-1})) d\omega = \\ &\int q(\omega) \log p\left(\mathbf{y}_T \left| \mathbf{f}_y^\omega(\mathbf{x}_T, \mathbf{f}_y^\omega(\mathbf{x}_{T-1}, \dots, \mathbf{f}_y^\omega(\mathbf{x}_1, \mathbf{y}_0) \dots)) \right.\right) d\omega \end{aligned}$$

where the dependence on  $\mathbf{c}_T$  was dropped for brevity. We approximate the last equation by Monte Carlo integration with a single sample. This allows us to rewrite eq. (3) as

$$\begin{aligned} \mathcal{L}_{VI} &= - \log p\left(\mathbf{y}_T \left| \mathbf{f}_y^{\hat{\omega}}(\mathbf{x}_T, \mathbf{f}_y^{\hat{\omega}}(\mathbf{x}_{T-1}, \dots, \mathbf{f}_y^{\hat{\omega}}(\mathbf{x}_1, \mathbf{y}_0) \dots)) \right.\right) \\ &\quad + \sum_{i=1}^L \frac{p_i l^2}{2N} (\|\mathbf{W}_i\|_2^2 + \|\mathbf{b}_i\|_2^2) \end{aligned}$$

<sup>2</sup>Related literature on RNNs with distributions over their weights includes (Bitzer & Kiebel, 2012; Chien & Ku, 2014; Graves, 2011)

<sup>3</sup>We define  $\mathbf{y}_0$  to be some constant value such as 0.

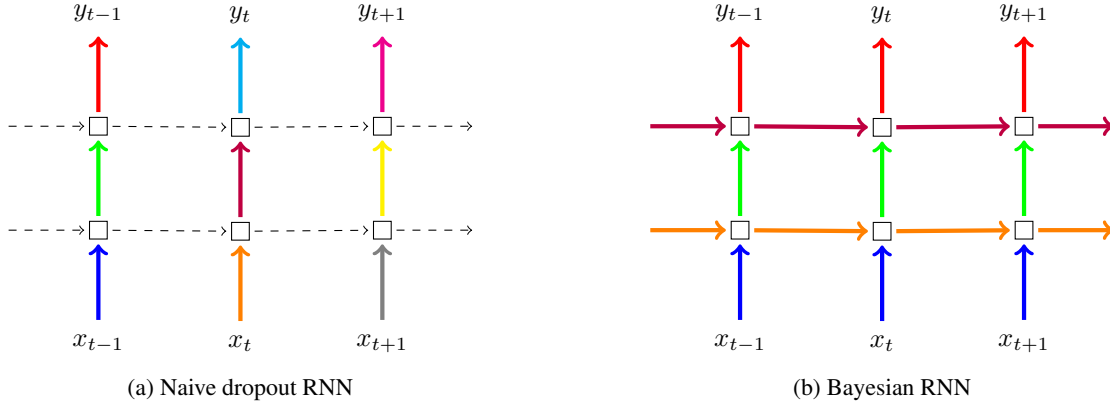


Figure 1. Depiction of the dropout technique following our Bayesian RNN interpretation (right) compared to the standard technique in the field (left). Each square represents an RNN unit, with horizontal arrows representing time dependence (recurrent connections). Vertical arrows represent the input and output to each RNN unit. Coloured connections represent dropped-out inputs, with different colours corresponding to different dropout masks. Dashed lines correspond to standard connections with no dropout. Current techniques (naive dropout, left) use different masks at different time steps, with no dropout on the recurrent layers. The proposed technique (Bayesian RNN, right) uses the same dropout mask at each time step, including the recurrent layers.

with  $\hat{\omega} \sim q(\omega)$  and prior length-scale  $l$ , defining our noisy objective. The second term in the objective (the KL to the prior) was approximated following (Gal & Ghahramani, 2015b). This objective is an unbiased estimator of eq. (3), and will have identical optima as the original equation. Note that the same sample  $\hat{\omega}$  is used as parameters for  $\mathbf{f}_y$  at all time steps.

### 3.1. Implementation and Relation to Dropout in RNNs

Implementing this approximate Bayesian RNN inference efficiently, we could choose  $q(\omega)$  to follow eq. (4). In this case one would sample a single mask of Bernoulli random variables once for each matrix in  $\omega$ . We then use the same mask throughout the function applications  $\mathbf{f}_c^\omega, \mathbf{f}_y^\omega$  at every time step.

This is identical to implementing dropout with the same network units dropped at each time step, randomly dropping inputs, outputs, and recurrent connections. This is in comparison to existing techniques, where different network units would be dropped at different time steps, and no dropout is applied to the recurrent connections.

Another key difference is that in our method one would use different dropout masks for different gates (even when the same input  $\mathbf{x}_t$  is used). This is because the approximating distribution is placed over the matrices rather than the inputs: we might drop certain columns in one weight matrix  $\mathbf{W}$  applied to  $\mathbf{x}_t$  and different columns in another matrix  $\mathbf{W}'$  applied to  $\mathbf{x}_t$ . This is in contrast to existing techniques in which elements of the vector  $\mathbf{x}_t$  are dropped once before it is passed to any of the gates.

The method, and its relation to existing techniques, is depicted in figure 1. See section B in the appendix for sample code.

### 3.2. Embedding Dropout

In datasets with continuous inputs we often apply dropout to the input layer – i.e. to the input vector itself. This is equivalent to placing a distribution over the weight matrix which follows the input and approximately integrating over it (the matrix is optimised and therefore prone to overfitting otherwise).

But for models with discrete inputs such as words (where every word is mapped to a continuous vector – a *word embedding*) this is seldom done. With word embeddings the input can be seen as either the word embedding itself, or, more conveniently, as a “one-hot” encoding (a vector of zeros with 1 at a single position). The product of the one-hot encoded vector with an embedding matrix  $\mathbf{W}_E \in \mathbb{R}^{D \times V}$  (where  $D$  is the embedding dimensionality and  $V$  is the number of words in the vocabulary) then gives a word embedding. Curiously, this parameter layer is the largest layer in most language applications, yet it is often not regularised. Since the embedding matrix is optimised it can lead to overfitting, and it is therefore desirable to apply dropout to the one-hot encoded vectors. This in effect is identical to *dropping words at random* throughout the input sentence, and can also be interpreted as encouraging the model to not “depend” on single words for its output.

Note that as before, we randomly set columns of the matrix  $\mathbf{W}_E \in \mathbb{R}^{D \times V}$  to zero. Since we repeat the same mask at each time step, we drop the same words throughout the sequence – i.e. we drop word types at random rather than word tokens (as an example, the sentence “the dog and the cat” might become “— dog and — cat” or “the — and the cat”, but never “— dog and the cat”). A possible inefficiency implementing this is the requirement to sample  $V$  Bernoulli random variables, where  $V$  might be large.



This can be solved by the observation that for sequences of length  $T$ , at most  $T$  embeddings could be dropped (other dropped embeddings have no effect on the model output). For  $T \ll V$  it is therefore more efficient to first map the words to the word embeddings, and only then to zero-out word embeddings based on their word type.

## 4. Experimental Evaluation

We evaluate the proposed technique on tasks of sentiment analysis and language modelling. The task of sentiment analysis demonstrates well the advantages of correct regularisation: labelled datasets are often small and expensive to collect. We compare our approach to standard techniques in the field, and study the performance of different dropout configurations, network structures (LSTM and GRU), and more. We then use a language modelling task on the Penn Treebank (Marcus et al., 1993) to assess our approach on a larger dataset. We compare our approach to the reference implementation of (Zaremba, Sutskever, and Vinyals, 2014) which has become standard in the field.

### 4.1. Sentiment Analysis

We use the raw Cornell film reviews corpus collected by Pang & Lee (2005). The dataset is composed of 5000 film reviews. We extract consecutive segments of  $T$  words from each review for  $T = 200$ , and use the corresponding film score as the observed output  $y$ . The model is built from one embedding layer (of dimensionality 128), one LSTM layer (with 128 network units for each gate; GRU is studied below), and finally a fully connected layer applied to the last output of the LSTM (resulting in a scalar output). We use the Adam optimiser (Kingma & Ba, 2014) throughout the experiments, with batch size 128, and MC dropout at

test time with 10 samples.

Throughout the experiments we refer to LSTMs with the dropout technique proposed following our Bayesian interpretation as *Bayesian LSTMs*, and refer to existing dropout techniques as *naive dropout LSTMs* (different masks at different steps, applied to the input and output of the LSTM alone). We refer to LSTMs with no dropout as *standard LSTMs*.

The main results can be seen in fig. 2. We compare a fully Bayesian LSTM (i.e. approximately integrating *all* parameter layers) to standard techniques in the field. For each model we used the best regularisation settings that avoid model overfitting. These are obtained by evaluating each model with dropout probabilities 0.25 and 0.5 (identical probabilities for all dropout layers), and weight decays ranging from  $10^{-6}$  to  $10^{-4}$ . The optimal setting for Bayesian LSTM seems to be dropout probabilities 0.25 and weight decay  $10^{-3}$ , and for naive dropout LSTM the dropout probabilities are 0.5 (no weight decay is used in reference implementations of naive dropout LSTM (Zaremba et al., 2014)). Convergence plots of the loss for each model are given in the appendix. It seems that the only model not to overfit is the Bayesian one, which achieves lowest test error as well. A study of the effects of various dropout settings in different layers in the Bayesian LSTM is given next.

### 4.2. Bayesian LSTM with Different Dropout Configurations

We assess our Bayesian LSTM with different combinations of dropout over the embeddings ( $p_E = 0, 0.5$ ) and recurrent layers ( $p_U = 0, 0.5$ ) on the same task as in the previous section. The results can be seen in figure 3. It seems that

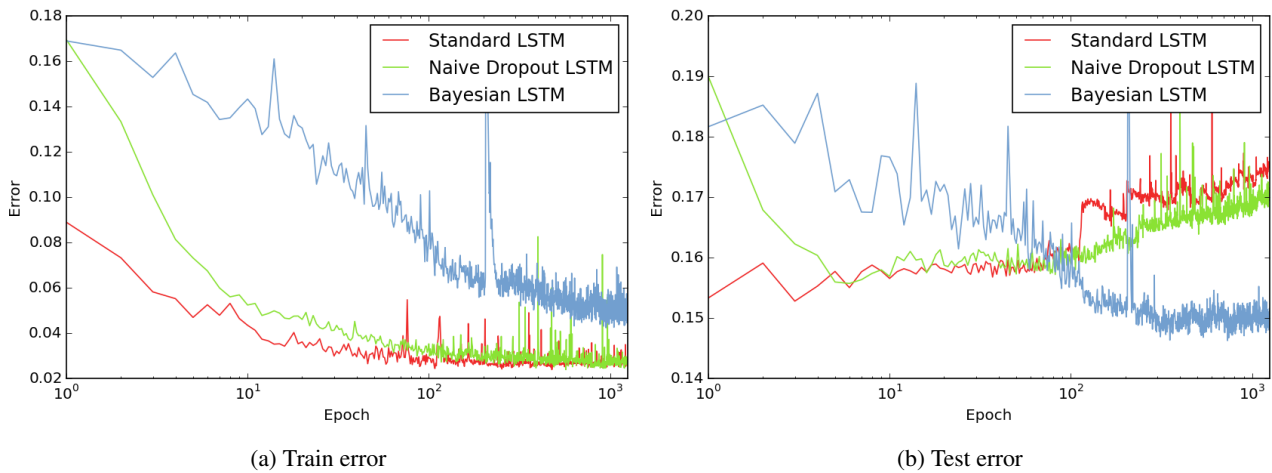


Figure 2. Sentiment analysis error for *Bayesian LSTM* (with dropout in recurrent layers and identical mask used for all steps) compared to *dropout LSTM* (as is used in the literature today) and *standard LSTM* (with no dropout). All models have converged, with Bayesian LSTM the only model not overfitting and achieving lowest error.

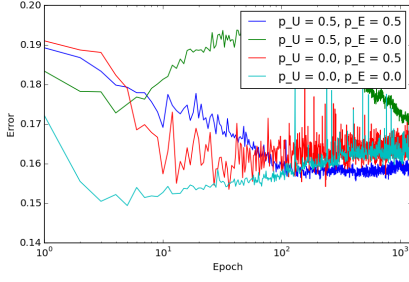


Figure 3. Test error for Bayesian LSTM with different dropout probabilities for the recurrent layer ( $p_U$ ) and embedding layer ( $p_E$ ).

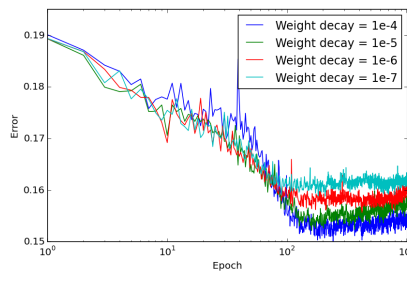


Figure 4. Test error for Bayesian LSTM with different weight decays.

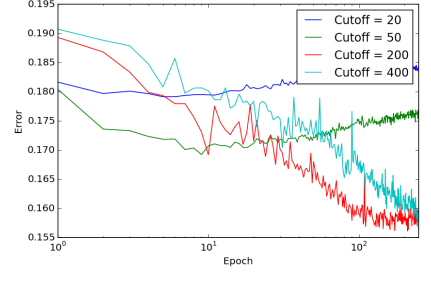


Figure 5. Bayesian LSTM test error for different sequence lengths ( $T = 20, 50, 200, 400$  cut-offs).

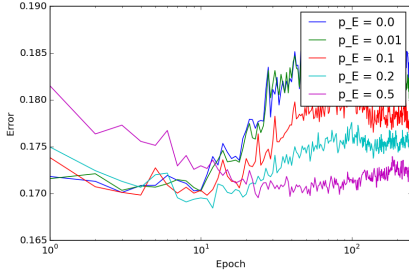


Figure 6. Test error for various embedding dropout probabilities, with sequence length 50.

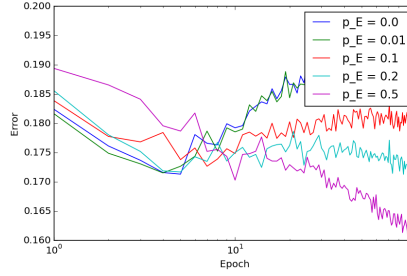


Figure 7. Test error for various embedding dropout probabilities, with sequence length 200.

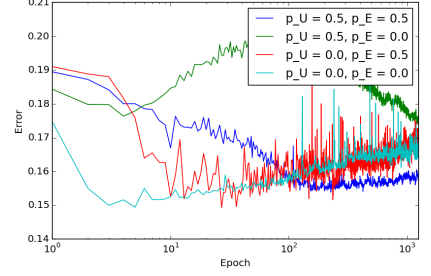
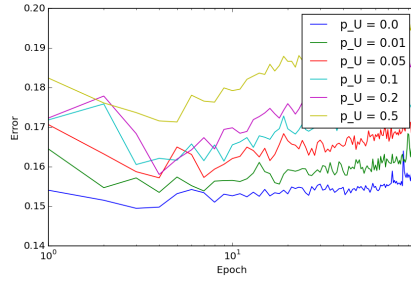
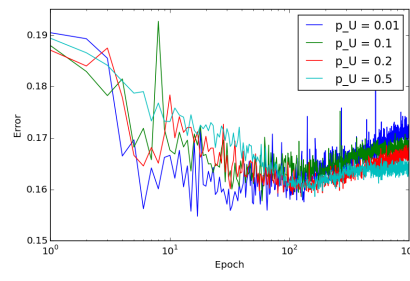


Figure 8. Dropout approximation in Bayesian LSTM with different dropout probabilities.



(a) Test error for  $p_E = 0$



(b) Test error for  $p_E = 0.5$

Figure 9. Test error for Bayesian LSTM with different dropout probabilities for the recurrent layer ( $p_U$ ) with a fixed embedding layer dropout probability ( $p_E = 0, 0.5$ ). Note that in this experiment we used weight decay  $10^{-10}$ , explaining the over-fitting for  $p_U = 0.5$ .

without both strong embeddings regularisation and strong regularisation over the recurrent layers the model would overfit rather quickly. The behaviour when  $p_U = 0.5$  and  $p_E = 0$  is quite interesting: test error decreases and then increases before decreasing again. Also, it seems that when  $p_U = 0$  and  $p_E = 0.5$  the model becomes very erratic.

We further tested the fully Bayesian LSTM model with different weight decays, observing the effects of different values for these. Note that weight decay is applied to all layers, including the embedding layer. In figure 4 we can see that higher weight decay values result in lower test error, with significant differences for different weight decays. This suggests that weight decay still plays an important role even when using dropout (whereas common practice is to remove weight decay with naive dropout). Note also

that the weight decay can be optimised (together with the dropout parameters) as part of the variational approximation. This is not done in practice in the deep learning community, where grid-search or Bayesian optimisation are often used for these instead.

Testing the Bayesian LSTM with different sequence lengths (with sequences of lengths  $T = 20, 50, 200, 400$ ) we can see that sequence length has a strong effect on model performance as well (fig. 5). Longer sequences result in much better performance but with the price of longer convergence time. We hypothesised that the diminished performance on shorter sequences is caused by the high dropout probability on the embeddings. But a follow-up experiment with sequence lengths 50 and 200, and different embedding dropout probabilities, shows that lower dropout

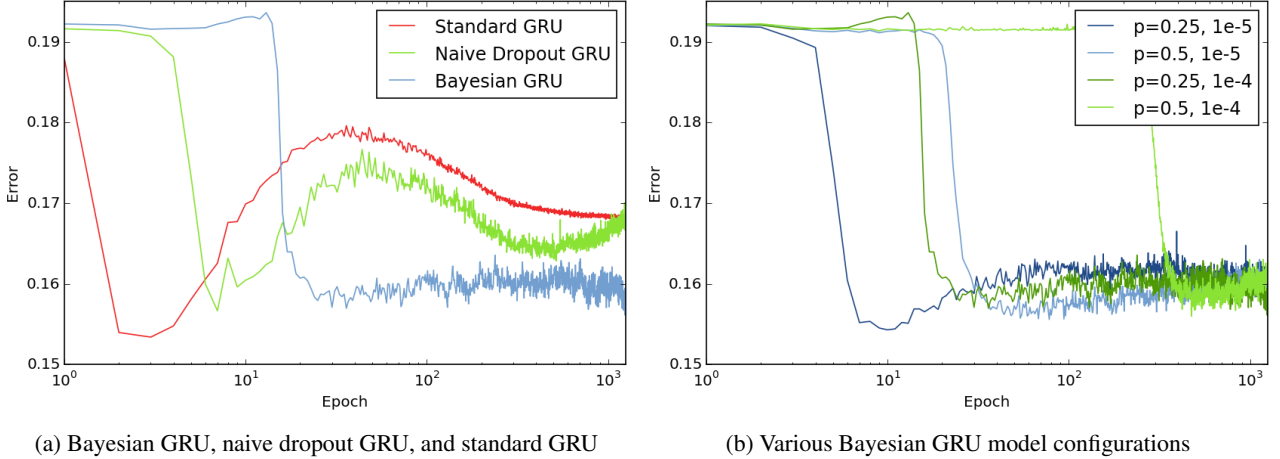


Figure 10. Sentiment analysis error for Bayesian GRU compared to naive dropout GRU and standard GRU (with no dropout). Test error for the different models (left) and for different Bayesian GRU configurations (right).

probabilities result in even worse model performance (figures 6 and 7).

Lastly, we tested the performance of the Bayesian LSTM with different recurrent layer dropout probabilities, fixing the embedding dropout probability at either  $p_E = 0$  or  $p_E = 0.5$  (fig. 9). These results are rather intriguing. In this experiment all models have converged, with the loss getting near zero (not shown). Yet it seems that with no embedding dropout, a higher dropout probability within the recurrent layers leads to overfitting! This presumably happens because of the large number of parameters in the embedding layer which is not regularised. Regularising the embedding layer with dropout probability  $p_E = 0.5$  we see that a higher recurrent layer dropout probability indeed leads to increased *robustness* to overfitting, as expected. These results suggest that embedding dropout can be of crucial importance in some tasks.

Further experiment evaluations are given in the appendix, together with loss plots of the various models above.

### 4.3. Dropout Approximation in Bayesian LSTMs

We next assess the *dropout approximation* in Bayesian LSTMs. The dropout approximation is often used in deep networks as means of approximating the MC estimate. In the approximation we replace each weight matrix  $\mathbf{M}$  by  $p\mathbf{M}$  where  $p$  is the dropout probability, and perform a deterministic pass through the network (without dropping out units). This can be seen as propagating the mean of the random variables  $\mathbf{W}$  through the network (Gal & Ghahramani, 2015b). The approximation has been shown to work well for deep networks (Srivastava et al., 2014), yet it fails with convolution layers (Gal & Ghahramani, 2015a). We assess the approximation empirically with our Bayesian LSTM model, repeating the first experiment with the approximation used at test time instead of MC dropout. The results can be seen in fig. 8. It seems that the approximation gives

a good estimate to the test error, similar to the results in figure 3. Further evaluation of the approximation is given in the appendix.

### 4.4. Bayesian GRU

We assessed the GRU network model as well, repeating the first experiment setup. Optimal dropout probabilities and weight decay were used again for each model. In fig. 10a we see that Bayesian GRU avoids overfitting to the data and converges to the lowest test error. In fig. 10b we see how different dropout probabilities and weight decays affect model performance. It is interesting to note that standard techniques exhibit peculiar behaviour where the test error repeatedly decreases and increases. This behaviour is not observed with the Bayesian GRU. It is also worth noting that lowest test error is obtained by the unregularised GRU model at the second epoch. Early stopping in this case will result in smaller test error, but will come with the additional cost of decreasing dataset size for cross-validation (where the dataset is already very small).

### 4.5. Language Modelling

For our final experiment, we replicate the experiment setup of Zaremba, Sutskever, and Vinyals (2014) on a language modelling task with the Penn Treebank. This dataset is larger than the previous one, with 887, 521 tokens in total. Following (Zaremba et al., 2014) we build a deep LSTM with 2 layers and 200 units in each layer. Our vocabulary size is 10,000 and we optimise the models with SGD for 180 epochs. We make two key changes to the setting of (Zaremba et al., 2014). First, we do not decay the learning rate. We noticed that the learning rate decay schedule in (Zaremba et al., 2014) was selected in such a way that ensures the gradient descent steps are small when the model starts overfitting. Removing this decay (or alternatively using a smaller decay) shows the naive dropout model’s ten-

|                  | Standard LSTM | Naive dropout LSTM | Bayesian LSTM |
|------------------|---------------|--------------------|---------------|
| Validation perp. | 290           | 148                | <b>126</b>    |
| Test perp.       | 273           | 131                | <b>115</b>    |

Table 1. Language model validation and test perplexities for best model configurations.

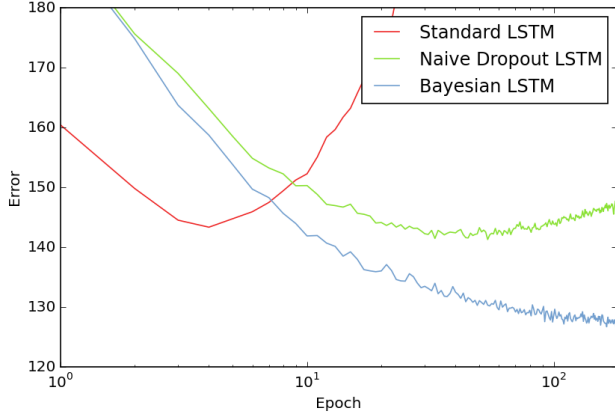


Figure 12. Language model validation perplexity on the Penn Treebank for Bayesian LSTM, naive dropout LSTM, and standard LSTM.

dency to overfit. Second, we initialise each sequence cell with 0 rather than the end state of the previous forward pass. This is to get a fair comparison of all models (standard dropout LSTM, naive dropout LSTM and Bayesian LSTM) which is not affected by various tricks. As before, we select the best configuration for each model that avoids model overfitting. For naive dropout LSTM this is dropout probability 0.5 (no weight decay is used in the reference implementation). For Bayesian LSTM this is dropout probability 0.25 with weight decay  $10^{-4}$ .

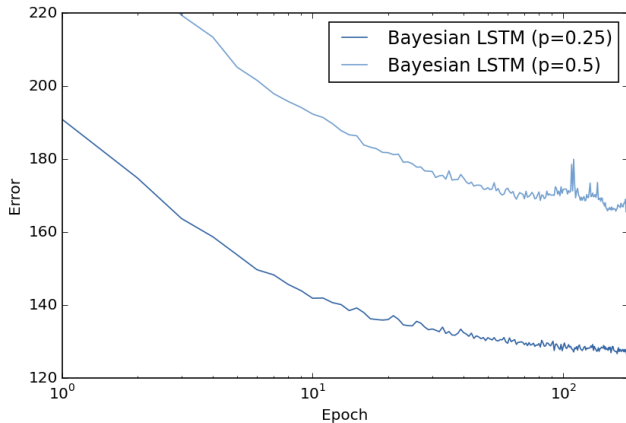
The main results of our experiment are shown in fig. 12. As can be seen, the Bayesian LSTM achieves lower validation perplexity (a measure of model confusion predicting the next word), with all other models overfitting. In

fig. 11 we show the validation perplexity of various model configurations for both naive dropout LSTM and Bayesian LSTM. Note that a lower dropout probability of 0.25 for naive dropout LSTM results in a lower validation perplexity (although the lowest point is still higher than Bayesian LSTM’s final validation perplexity), but also increased overfitting. This is because the model regularisation is weaker. A quantitative comparison of all models is given in table 1. In the table we report validation perplexity as well as test perplexity. This confirms our observations from the validation perplexity plots.

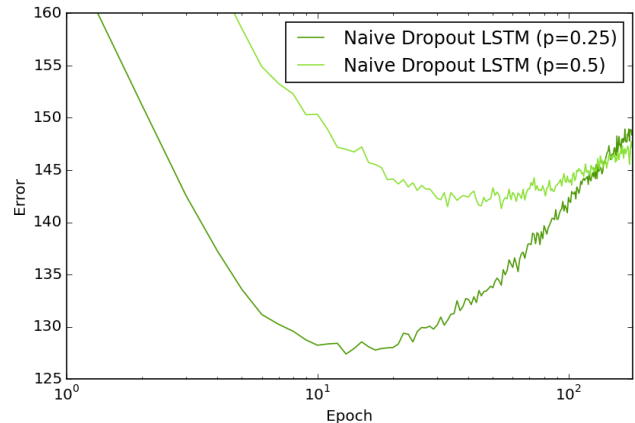
## 5. Discussion and Future Research

We’ve seen how theoretical developments can lead to new tools within deep learning, solving a major problem with existing sequence models. Compared to existing pragmatic approaches in the field, where empirical experimentation with various tools might lead to new findings, we developed a hypothesis trying to understand why existing tools work well. In an attempt to validate or falsify the hypothesis we made *predictions* (in the scientific sense) which we evaluated empirically. The results in this paper seem to offer further evidence for the theory suggested in (Gal & Ghahramani, 2015b), extending on the evidence accumulated in (Gal & Ghahramani, 2015a), and extending the arsenal of variational tools in deep learning.

In future research we aim to assess model uncertainty in Bayesian LSTMs. Together with the developments presented here, this will have important implications for modelling language ambiguity.



(a) Bayesian LSTM



(b) Naive dropout LSTM

Figure 11. Language model validation perplexity for different model configurations.



## References

- Barber, David and Bishop, Christopher M. Ensemble learning in Bayesian neural networks. *NATO ASI SERIES F COMPUTER AND SYSTEMS SCIENCES*, 168:215–238, 1998.
- Bayer, Justin, Osendorfer, Christian, Korhammer, Daniela, Chen, Nutan, Urban, Sebastian, and van der Smagt, Patrick. On fast dropout and its applicability to recurrent networks. *arXiv preprint arXiv:1311.0701*, 2013.
- Bergstra, James, Breuleux, Olivier, Bastien, Frédéric, Lamblin, Pascal, Pascanu, Razvan, Desjardins, Guillaume, Turian, Joseph, Warde-Farley, David, and Bengio, Yoshua. Theano: a CPU and GPU math expression compiler. In *Proceedings of the Python for Scientific Computing Conference (SciPy)*, June 2010. Oral Presentation.
- Bitzer, Sebastian and Kiebel, Stefan J. Recognizing recurrent neural networks (rRNN): Bayesian inference for recurrent neural networks. *Biological cybernetics*, 106(4-5):201–217, 2012.
- Bluche, Théodore, Kermorvant, Christopher, and Louradour, Jérôme. Where to apply dropout in recurrent neural networks for handwriting recognition? In *Document Analysis and Recognition (ICDAR), 2015 13th International Conference on*, pp. 681–685. IEEE, 2015.
- Blundell, Charles, Cornebise, Julien, Kavukcuoglu, Koray, and Wierstra, Daan. Weight uncertainty in neural networks. *arXiv preprint arXiv:1505.05424*, 2015.
- Chien, Jen-Tzung and Ku, Yuan-Chu. Bayesian recurrent neural network language model. In *Spoken Language Technology Workshop (SLT), 2014 IEEE*, pp. 206–211. IEEE, 2014.
- Cho, Kyunghyun, van Merriënboer, Bart, Gulcehre, Caglar, Bahdanau, Dzmitry, Bougares, Fethi, Schwenk, Holger, and Bengio, Yoshua. Learning phrase representations using RNN encoder–decoder for statistical machine translation. In *Proceedings of the 2014 Conference on Empirical Methods in Natural Language Processing (EMNLP)*, pp. 1724–1734, Doha, Qatar, October 2014. Association for Computational Linguistics.
- fchollet. Keras. <https://github.com/fchollet/keras>, 2015.
- Gal, Yarin and Ghahramani, Zoubin. Bayesian convolutional neural networks with Bernoulli approximate variational inference. *arXiv:1506.02158*, 2015a.
- Gal, Yarin and Ghahramani, Zoubin. Dropout as a Bayesian approximation: Representing model uncertainty in deep learning. *arXiv:1506.02142*, 2015b.
- Graves, Alex. Practical variational inference for neural networks. In *Advances in Neural Information Processing Systems*, pp. 2348–2356, 2011.
- Hinton, Geoffrey E and Van Camp, Drew. Keeping the neural networks simple by minimizing the description length of the weights. In *Proceedings of the sixth annual conference on Computational learning theory*, pp. 5–13. ACM, 1993.
- Hinton, Geoffrey E, Srivastava, Nitish, Krizhevsky, Alex, Sutskever, Ilya, and Salakhutdinov, Ruslan R. Improving neural networks by preventing co-adaptation of feature detectors. *arXiv preprint arXiv:1207.0580*, 2012.
- Hochreiter, Sepp and Schmidhuber, Jürgen. Long short-term memory. *Neural computation*, 9(8):1735–1780, 1997.
- Kalchbrenner, Nal and Blunsom, Phil. Recurrent continuous translation models. In *EMNLP*, pp. 1700–1709, 2013.
- Kingma, Diederik and Ba, Jimmy. Adam: A method for stochastic optimization. *arXiv preprint arXiv:1412.6980*, 2014.
- Marcus, Mitchell P, Marcinkiewicz, Mary Ann, and Santorini, Beatrice. Building a large annotated corpus of english: The Penn Treebank. *Computational linguistics*, 19(2):313–330, 1993.
- Pachitariu, Marius and Sahani, Maneesh. Regularization and nonlinearities for neural language models: when are they needed? *arXiv preprint arXiv:1301.5650*, 2013.
- Pang, Bo and Lee, Lillian. Seeing stars: Exploiting class relationships for sentiment categorization with respect to rating scales. In *Proceedings of the 43rd Annual Meeting on Association for Computational Linguistics*, pp. 115–124. Association for Computational Linguistics, 2005. URL [cornell.edu/people/pabo/movie-review-data/](http://cornell.edu/people/pabo/movie-review-data/).
- Pham, Vu, Bluche, Theodore, Kermorvant, Christopher, and Louradour, Jerome. Dropout improves recurrent neural networks for handwriting recognition. In *2014 14th International Conference on Frontiers in Handwriting Recognition (ICFHR)*, pp. 285–290. IEEE, 2014.
- Srivastava, Nitish, Hinton, Geoffrey, Krizhevsky, Alex, Sutskever, Ilya, and Salakhutdinov, Ruslan. Dropout: A simple way to prevent neural networks from overfitting. *The Journal of Machine Learning Research*, 15(1): 1929–1958, 2014.

Sundermeyer, Martin, Schlüter, Ralf, and Ney, Hermann.  
LSTM neural networks for language modeling. In *INTERSPEECH*, 2012.

Sutskever, Ilya, Vinyals, Oriol, and Le, Quoc VV. Sequence to sequence learning with neural networks. In *Advances in neural information processing systems*, pp. 3104–3112, 2014.

Zaremba, Wojciech, Sutskever, Ilya, and Vinyals, Oriol.  
Recurrent neural network regularization. *arXiv preprint arXiv:1409.2329*, 2014.

## A. Further results

We compare naive dropout LSTM to Bayesian LSTM with dropout probability in the recurrent layers set to zero:  $p_U = 0$  (referred to as *dropout LSTM*). Both models apply dropout to the input and outputs of the LSTM alone, with no dropout applied to the embeddings. Naive dropout LSTM uses different masks at different time steps though, tied across the gates, whereas dropout LSTM uses the same mask at different time steps. The test error for both models can be seen in fig. 13. It seems that without dropout over the recurrent layers and embeddings both models overfit, and in fact result in identical performance.

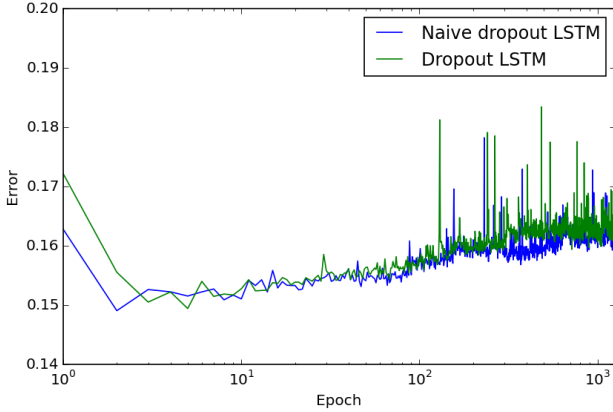


Figure 13. Naive dropout LSTM uses different dropout masks at each time step, whereas Dropout LSTM uses the same mask at each time step. Both models apply dropout to the inputs and outputs alone, and result in identical performance.

Next, we plot the train loss for various models from the main body of the paper. All models have converged, with a stable train loss.

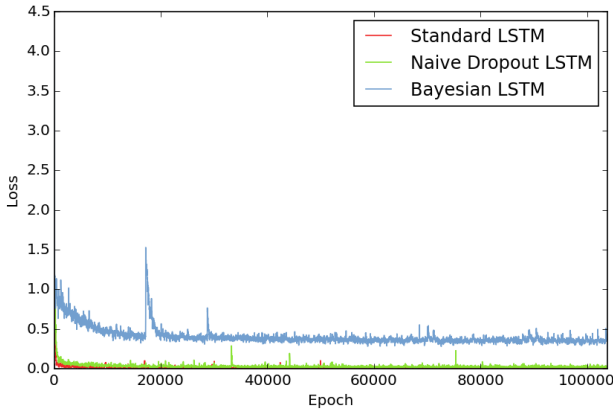


Figure 14. Train loss (as a function of batches) for figure 2

We assess the dropout approximation in the GRU model as well. The approximation seems to give similar results to

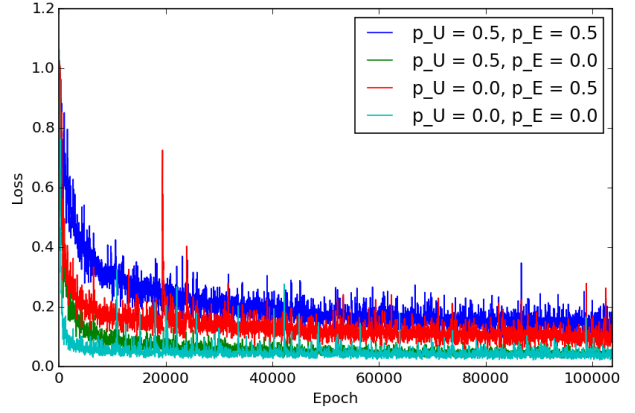


Figure 15. Train loss (as a function of batches) for figure 3

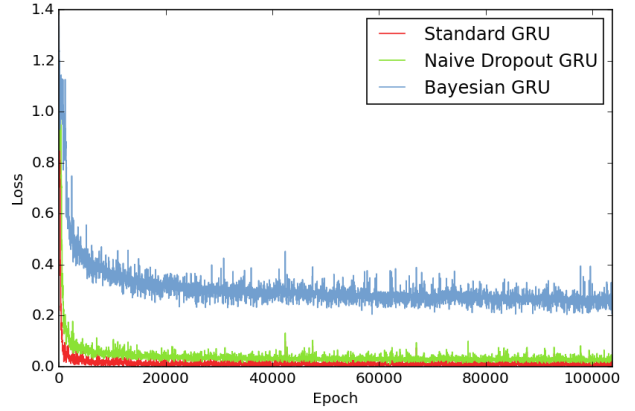


Figure 16. GRU train loss (as a function of batches) (figure 10a)

MC dropout in the GRU model:

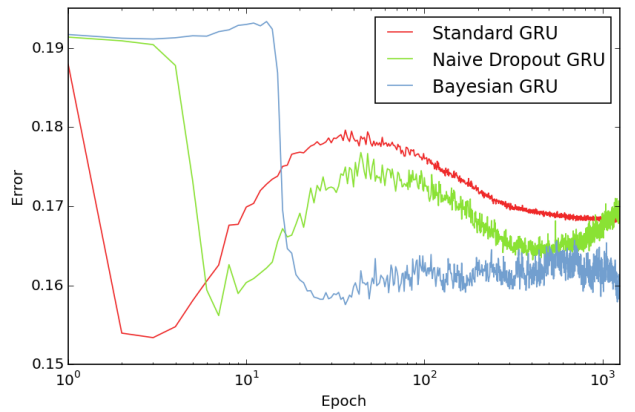


Figure 17. GRU dropout approximation

Lastly, we give the train perplexity plot for the language model experiment:

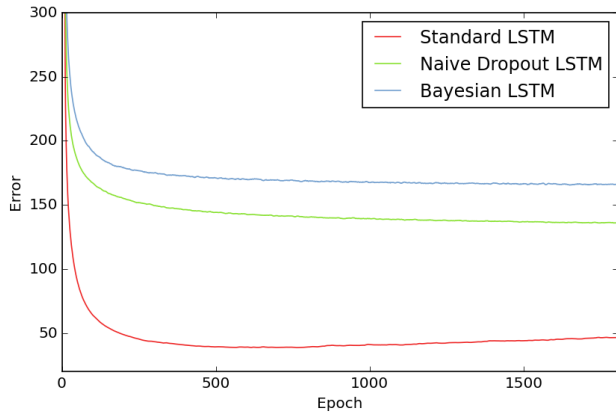


Figure 18. Language model train perplexity for Bayesian LSTM, naive dropout LSTM, and standard LSTM

## B. Code

An efficient Theano ([Bergstra et al., 2010](#)) implementation of the method above into Keras ([fchollet, 2015](#)) is as simple as:

```
def get_output(self, train=False):
    X = self.get_input(train)

    retain_prob_W = 1. - self.p_W[0]
    retain_prob_U = 1. - self.p_U[0]
    B_W = self.srng.binomial((4, X.shape[1], self.input_dim),
                             p=retain_prob_W, dtype=theano.config.floatX)
    B_U = self.srng.binomial((4, X.shape[1], self.output_dim),
                             p=retain_prob_U, dtype=theano.config.floatX)

    xi = T.dot(X * B_W[0], self.W_i) + self.b_i
    xf = T.dot(X * B_W[1], self.W_f) + self.b_f
    xc = T.dot(X * B_W[2], self.W_c) + self.b_c
    xo = T.dot(X * B_W[3], self.W_o) + self.b_o

    [outputs, memories], updates = theano.scan(
        self._step,
        sequences=[xi, xf, xo, xc],
        outputs_info=[
            T.unbroadcast(alloc_zeros_matrix(X.shape[1], self.output_dim), 1),
            T.unbroadcast(alloc_zeros_matrix(X.shape[1], self.output_dim), 1)
        ],
        non_sequences=[self.U_i, self.U_f, self.U_o, self.U_c, B_U],
        truncate_gradient=self.truncate_gradient)

    return outputs[-1]

def _step(self,
          xi_t, xf_t, xo_t, xc_t,
          h_tm1, c_tm1,
          u_i, u_f, u_o, u_c, B_U):
    i_t = self.inner_activation(xi_t + T.dot(h_tm1 * B_U[0], u_i))
    f_t = self.inner_activation(xf_t + T.dot(h_tm1 * B_U[1], u_f))
    c_t = f_t * c_tm1 + i_t * self.activation(xc_t + T.dot(h_tm1 * B_U[2], u_c))
    o_t = self.inner_activation(xo_t + T.dot(h_tm1 * B_U[3], u_o))
    h_t = o_t * self.activation(c_t)
    return h_t, c_t
```